Estimation of Delamination Crack Depth using Passive Thermography

Joseph N. Zalameda*, Wade C. Jackson, and Cheryl A. Rose

NASA Langley Research Center Hampton, VA 23681-2199

ABSTRACT

Passive thermography is used to monitor small increases in temperature resulting from delamination damage formation in a composite hat-stiffened panel during quasi-static loading. The heating is composed of two heat generation components. The first component is an instantaneous response due to a strain release during quasi-static loading. The second component is mechanical heating, at the interface of failure, due to fracture damage. This second component produces a transient rise in temperature that is a function of the damage depth and thermal diffusivity. The first component defines the thermal start time for the transient response. A one-dimensional thermal model is used to determine the damage depth. The results are compared to ultrasonic and X-ray CT data. The advantages and limitations of the thermal technique for damage depth detection are discussed.

Keywords: Thermal nondestructive evaluation, passive thermography, quasi-static load damage detection, delamination damage, crack depth, X-ray computed tomography, non-immersion ultrasound

1. INTRODUCTION

Passive thermography is similar to active thermography as both techniques rely on detecting small surface temperature differences due to applied or removed energy. Active thermography implies the energy for the inspection is controlled. For example, delivery of heating using a lamp where start time, duration, and amount of energy delivered for the purposes of the inspection are controlled. Passive thermography implies no control of the applied energy such as the sun, hot air, moisture evaporation, or structural loading. The infrared camera passively records the thermal imagery. Passive thermography is used for real-time nondestructive evaluation (NDE) of a composite structure during quasi-static loading. Real time NDE is necessary for composites load testing to track early onset and growth of damage. The NDE allows for monitoring, and hence, controlling the growth of the damage as a function of the applied load. When damage is detected, the loading is stopped and other inspection techniques such as ultrasound and X-ray computed tomography (CT) are used to provide a detailed assessment of the panel damage as a function of depth and this information is used to feed damage prediction models [1,2]. The challenges for passive thermography are to detect the small, transient thermal signals generated during the quasi-static loading and to characterize the damage [3-6].

In this work, a quasi-static bending load (using seven contact points) is applied to a single stringer stiffened composite panel. Passive thermography is used to monitor the structure during load testing. Any small increases in temperature resulting from delamination damage formation in the panel during quasi-static loading are monitored in real time while the thermal data is recorded. It has been observed that the temperature rise at the surface is composed of two thermal responses. The first response is instantaneous and conforms to the shape of the damage. This instantaneous temperature rise is due to the thermoelastic release of energy when the sample fails over the area of failure [6,7]. The second response is a transient increase in temperature due to mechanical heating at the interface of failure [8]. This second component produces a transient rise in temperature that is a function of the damage depth and thermal diffusivity. The first component defines the thermal start time for the transient response. A one-dimensional thermal model is used to determine the damage depth for a given known thermal diffusivity. The results are compared to ultrasound and X-ray CT data. The advantages and limitations of the thermal technique for damage depth detection are discussed.

*joseph.n.zalameda@nasa.gov; phone 1 757-864-4793; fax 1 757-864-4914; http://nde.larc.nasa.gov

2. SAMPLE DESCRIPTION AND MEASUREMENT SYSTEMS

2.1 Composite Sample Tested

The stiffened composite panel skin was made up of 12 plies with a total thickness of 0.22 cm, the stiffener flange was made up of 12 plies with a total thickness of 0.24 cm. The stiffener hat top was made up of 16 plies with a total thickness of 0.32 cm. The stiffener was a woven composite. Figures 1a, 1b, and 1c show the stiffened composite panel stringer side, a painted specimen, and a cross sectional view respectively. The panel was painted for digital image correlation measurements to record panel deformation. Quasi-static loads were applied using seven application points, two on top (located in middle just outside of the flange) and five on the bottom (located at each corner and center). The load was applied from the bottom while the top was held stationary at two contact points. This configuration allowed for panel deformation that resulted in damage formation between the stiffener flange and skin. The applied quasi-static loads were up to 1,000 pounds. Examples of the applied load for a typical test and panel deflection are shown in Figures 2a and 2b respectively.

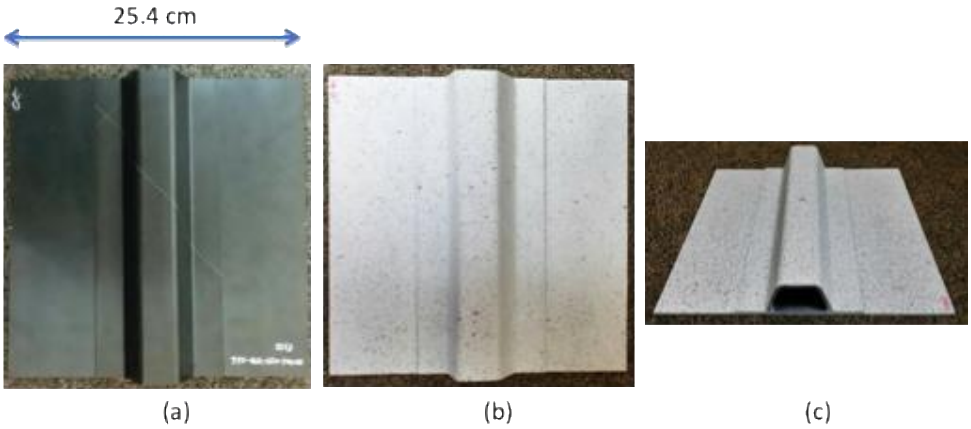

Figure 1: Single stringer composite panel with acoustic emission sensor locations.

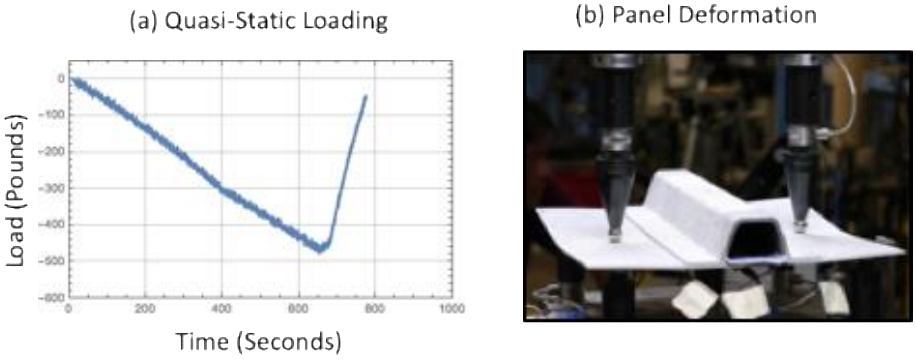

Figure 2: Applied load and panel deformation.

2.2 Passive Thermography

Passive thermography was used to track damage on the stringer side. The test setup is shown in Figure 3a along with an example infrared camera view shown in Figure 3b. The basic system consists of an IR camera operating in the 3–5 micrometer IR band and an image data acquisition computer. The IR camera was configured with 25 mm germanium optics. The focal plane array size of the camera was 640x512. The passive inspection captured the thermal variations

during the quasi-static loading. The setup required a Plexiglas® shield to filter out spurious IR background sources (not shown in Figure 3a). The camera frame rate was externally triggered and operated from frequencies of 80 to 180 Hz. The load signal was also acquired using a USB based 12-bit data acquisition module. For each infrared camera frame, a load value was acquired. Furthermore, real time averaging, a delayed image subtraction, and real time contrast adjustment were used to enhance detection of the small thermal transient signatures due to the damage [6]. Without this processing, the faint thermal signatures that indicate early damage would be difficult to nearly impossible to detect in real time. A typical test would last 25 minutes and 50 – 60 gigabytes of thermal data would be acquired for each run. When damage is detected the loading is stopped and the sample is removed for further damage characterization using ultrasound or X-ray CT.

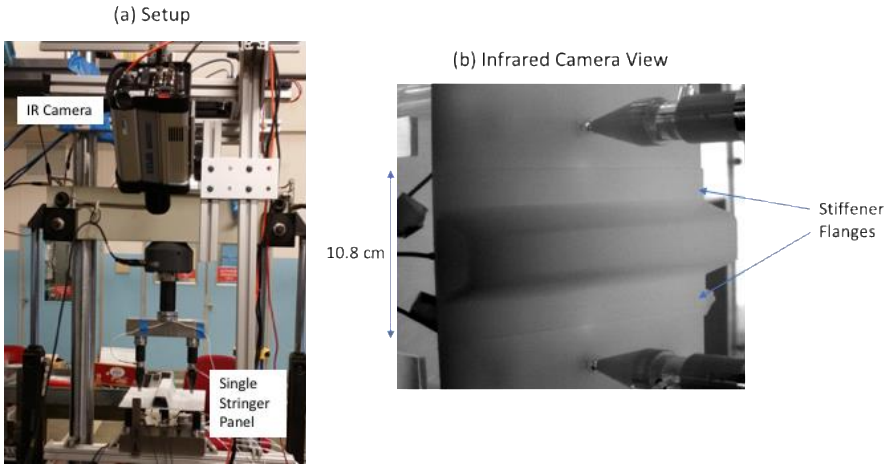

Figure 3: Quasi-static load test setup with infrared camera view.

3. MEASUREMENT RESULTS

3.1 Passive Thermography Data

Digital image processing was required to both enhance detection of thermal events during load and to facilitate comparison of the thermal inspection imagery to the ultrasonic or X-ray CT data. Typical parameters of 10 frames were averaged and a delay subtraction between the most recent averaged frame and the 100th averaged frame were used for real time processing to produce the output image. The delayed subtraction removed fixed background infrared radiation while increasing sensitivity to changes. Additionally, for comparison to ultrasonic data, an image perspective transformation was used. The image perspective transformation was used to correct for the infrared camera view angle since the optical line of sight was not normal. The image correction is performed by defining 4 points mapped to a new set of 4 desired points (normal view) [9].

Figure 4 shows the instantaneous thermal response where at 0.125 seconds the thermally detected damage is similar in size and shape to the ultrasonic inspection. The thermal data was acquired at 80 Hz for the small delamination. Each averaged frame represented 0.125 seconds. The damage is semi-elliptical as confirmed by both the thermal and ultrasonic inspection images. The instantaneous heating component can be seen more clearly in Figure 5 where a single pixel is plotted over the damaged region as a function of time. The instantaneous surface temperature increase occurs at approximately 79.8 seconds. Afterwards, there is a significant transient increase in temperature occurring around 81.0 seconds. This heating is due to the mechanical heating or heat flux generated at the failure interface. This heat diffuses to the surface and the thermal time to reach maximum temperature is a function of damage depth and thermal diffusivity. Similarly, in Figure 6, the instantaneous thermal response for the large area of failure is shown where at 0.056 seconds the thermally detected damage is similar in size and shape to the ultrasonic inspection. The thermal data was acquired at 180 Hz for the large delamination. Each averaged frame represented 0.056 seconds. The instantaneous heating component can be seen more clearly in Figure 7 where a single pixel is plotted over the damaged region as a function of time. The instantaneous surface temperature increase occurs at approximately 41.7 seconds. Afterwards there is a dominant transient increase in temperature occurring around 43 seconds.

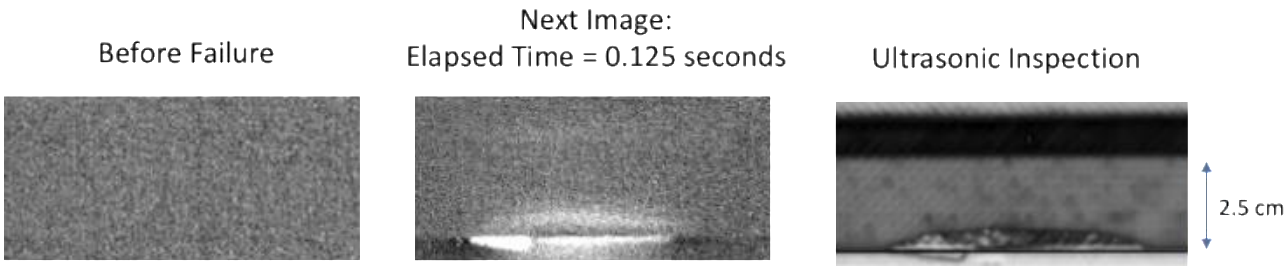

Figure 4: Comparison of instantaneous heating image to ultrasonic inspection for small delamination.

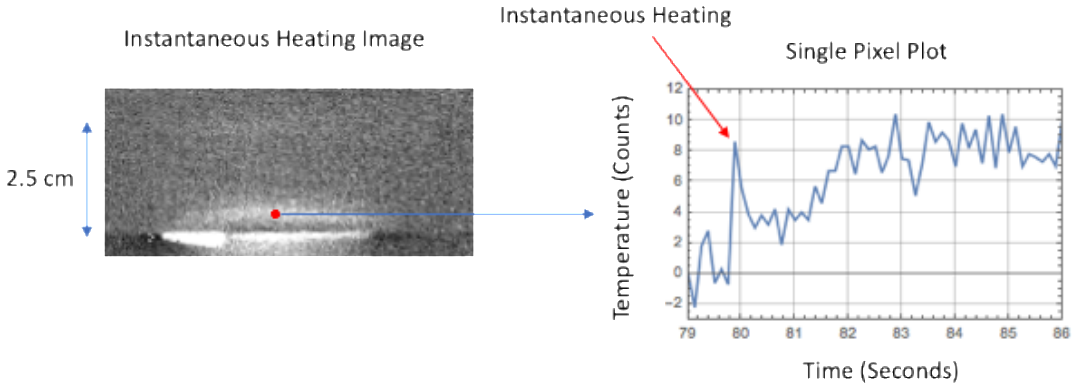

Figure 5: Single pixel plot of surface heating showing instantaneous heating response for small delamination.

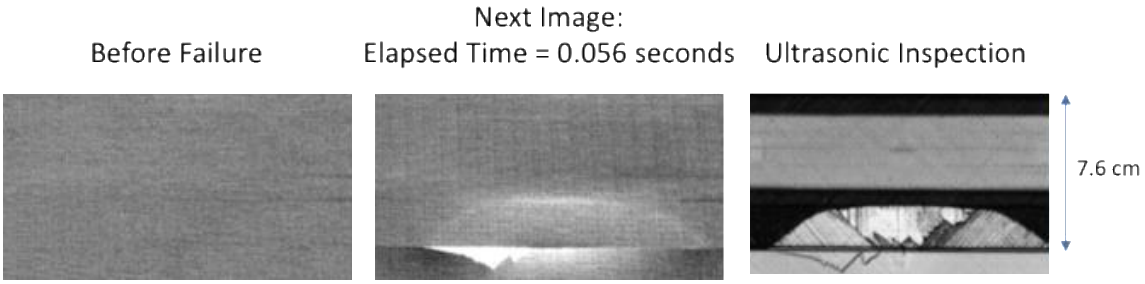

Figure 6: Comparison of instantaneous heating image to ultrasonic inspection for large delamination.

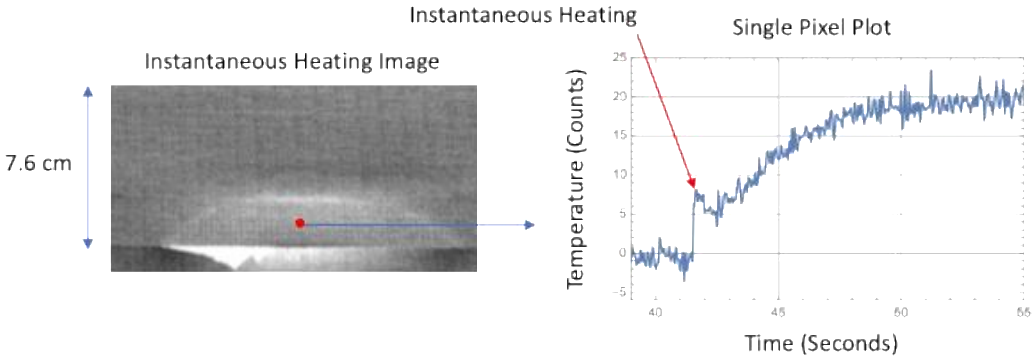

Figure 7: Single pixel plot of surface heating showing instantaneous heating response for large delamination.

4. DELAMINATION CRACK DEPTH ESTIMATION

4.1 Thermal Model

A delamination is most likely to form where the stiffener flange is attached to the skin as shown in Figure 8. The heat flux is created at the interface of failure. The heat flux is created due to the mechanical failure when the two surfaces separate. The separation is instantaneous and is modeled as an impulse heat flux that creates heating within the separated inner layers. Since the two layers are not in contact after failure, a simple two sided or through-transmission heat flow model is used. The depth of the damage is determined by the heat transfer from the inside to the outer surface. This temperature response will be a function of the damage depth and thermal diffusivity. A simple one-dimensional two-sided thermal measurement model can be used to estimate the damage depth if the thermal diffusivity is known.

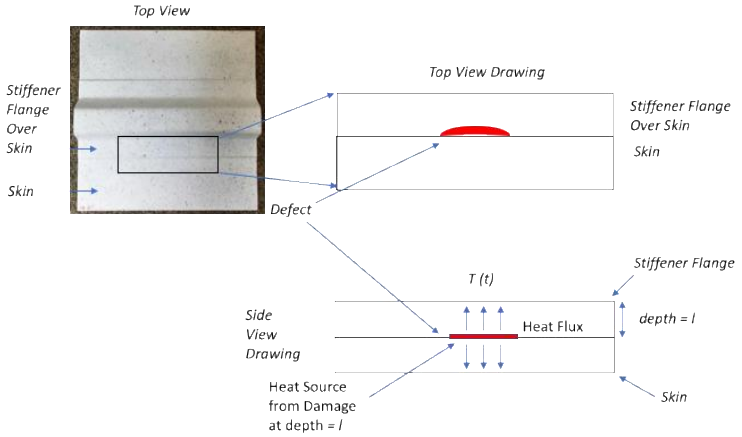

Figure 8: Diagram of damage formation on the hat stiffened composite panel.

The analytic solution derived by Winfree [10] is shown in equation (1). This equation is commonly used for a two-sided thermal measurement and is computationally efficient, when curve fitting, as compared to an infinite series solution [11].

$$T(t) = 2\,T_f\sqrt{\frac{l^2}{\alpha\,\pi\,t}}\left(\exp^{\frac{-l^2}{4\,\alpha\,t}} + \exp^{\frac{-9\,l^2}{4\,\alpha\,t}}\right) for\ t < 0.4\,\frac{l^2}{\alpha} \text{ and } T(t) = T_f\left(1 - 2\exp^{\frac{-\alpha\,\pi^2\,t}{l^2}}\right) for\ t \geq 0.4\,\frac{l^2}{\alpha} \quad (1)$$

T(t) is the surface temperature response, T_F is the final temperature, α is the thermal diffusivity, l is the layer thickness, and t is time. The temperature response equation assumes no convection losses and the heat flux generated is considered instantaneous for the samples inspected. The equation also does not take into account the instantaneous heating response, however the start time is determined from the instantaneous response. For a known thermal diffusivity, equation (1) was used to determine the damage depth, pixel by pixel, by minimizing the squared difference between the model and measured thermal response. A two parameter fit of the final temperature T_F and thickness l (damage depth) was implemented using the Levenberg-Marquardt curve fitting algorithm [12].

4.2 Comparison of Model to Data for Damage Depth

For a known thermal diffusivity, equation (1) was used to reduce the thermal data into a thickness image by fitting the thermal data pixel by pixel. The thermal diffusivity of the woven composite flange was measured previously using a two-sided thermal flash technique [10]. The thermal diffusivity value measured was 0.0042 cm^2/sec. Shown in Figures 9 and 10 are example model fit to the thermal data for a single pixel point (located in the damage center) for the small delamination and large delamination respectively. The data used for the model fit was truncated to remove the early times which is dominated by the instantaneous heating response. For example, for the small delamination, the fitting times were from approximately 0.9 to 7.5 seconds. The large delamination fitting times were from approximately 1.9 to 10 seconds. The thickness values obtained from the single pixel fit were 0.19 and 0.27 cm for the small and large delamination damage

respectively. By fitting the thermal model to the data pixel by pixel, the thermal data can be reduced to a thickness image revealing the damage depth. This is shown in Figures 11 and 12 for both the small delamination and large delamination.

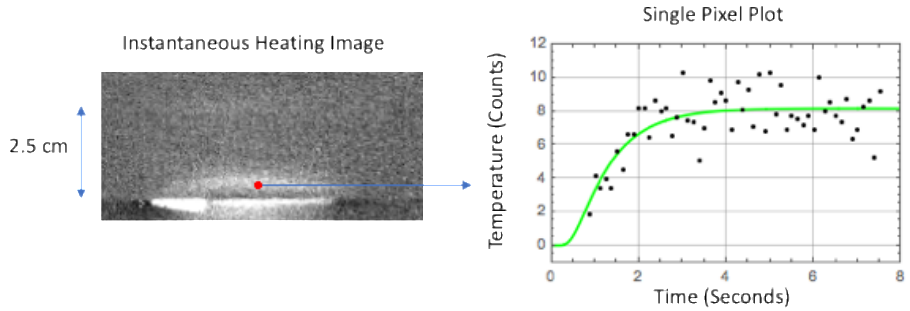

Figure 9: Temporal pixel plot comparison of thermal data to model for small delamination.

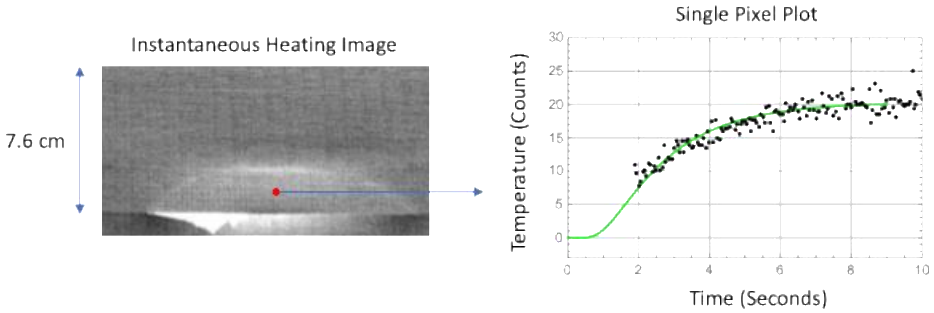

Figure 10: Temporal pixel plot comparison of thermal data to model for large delamination.

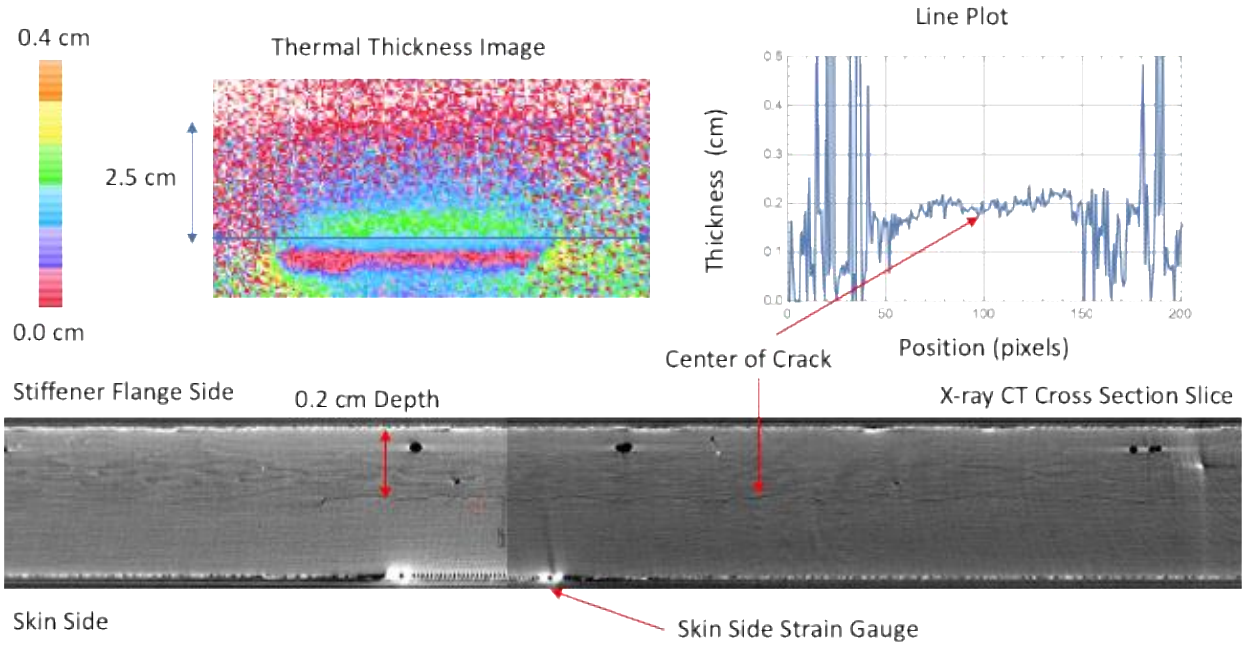

Figure 11: Thermally measured damage depth image and line plot for small delamination with comparison to X-ray CT cross section slice.

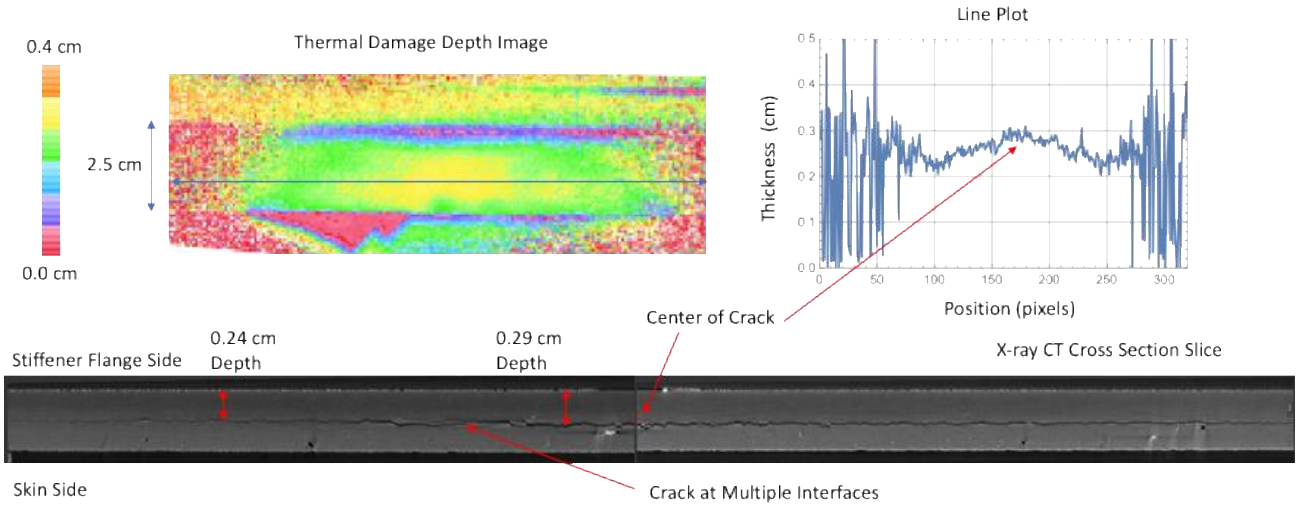

Figure 12: Thermally measured damage depth image and line plot for large delamination with comparison to X-ray CT cross section slice.

Also shown in Figures 11 and 12 are the respective line plots and X-ray CT cross section imagery. For the small delamination, the crack depth is measured approximately 0.1 cm from the edge of the stiffener flange toward the hat. The thermally measured depth appears uniform in depth at around 0.2 cm over the damaged area. This is confirmed from the X-ray CT image which shows a single crack around 0.2 cm in depth with no damage at other interfaces. Also note the thermally measured thickness away from the damage gives erroneous values due to the lack of a thermal response. For the large delamination, the crack depth is measured approximately 1.0 cm from the edge of the stiffener flange toward the hat. The thermally measured depth is not uniform in depth and varies over the damaged area from approximately 0.23 – 0.30 cm in depth with the deeper damage in the middle. This is confirmed from the X-ray CT image which shows a dominant crack around 0.24 – 0.29 cm in depth with the deeper damage at the center region. The X-ray CT image also reveals some damage at other interfaces in the center region which cannot be detected using this thermal technique. This is a limitation because the multi-layered damage cannot be accounted for using the single layer thermal model, however this could be studied with a more sophisticated thermal model in the future.

5. CONCLUSIONS

Passive thermography has been shown to be an effective real time NDE inspection technique to track damage onset and growth in a composite single stringer test panel during quasi-static loading in real time. The small transient thermal indications, detected with real time image processing, allowed for successful capture of damage initiation and growth. It has been observed that during delamination formation, the thermal response at the surface is composed of two signals. The first is an instantaneous temperature rise which is due to the thermoelastic release of energy when the sample fails over the area of failure. The instantaneous response is in good agreement with the size and shape of the ultrasound inspection. The second response is a transient increase in temperature due to the buried heat generated at the interface of failure. Using these two components, the damage depth can be imaged thermally and damage at different depths were detected. This could potentially help structural test engineers by providing damage location, size and depth during composites load testing.

REFERENCES

[1] Rose, C.A.; Dávila, C.G.; Leone, F.A. *Analysis Methods for Progressive Damage of Composite Structures*; NASA/TM-2013-218024; NASA Langley Research Center: Hampton, VA, USA, 2013.

[2] Clay, S. How ready are progressive damage analysis tools? *Compos. World* **2017**, *3*, 8–10.
[3] Roche, J.-M.; Balageas, D.; Lapeyronnie, B.; Passilly, F.; Mavel, A. Use of infrared thermography for in situ damage monitoring in woven composites. In Proceedings of the Photomechanics Conference 2013, Montpellier, France, 27–29 May 2013.
[4] Roche, J.-M.; Balageas, D.; Lamboul, B.; Bai, G.; Passilly, F.; Mavel, A.; Grail, G. Passive and active thermography for in situ damage monitoring in woven composites during mechanical testing. In Proceedings of the 39th Annual Review of Progress in Quantitative Nondestructive Evaluation, Baltimore, MD, USA, 21–26 July 2013; pp. 555–562.
[5] Zalameda, J.N., Horne, M.R. Real Time Detection of Damage during Quasi-Static Loading of a Single Stringer Panel using Passive Thermography. *Proc. SPIE* **2018**, 106610H, doi:10.1117/12.2305613.
[6] Zalameda, J.; Winfree, W. Detection and Characterization of Damage in Quasi-Static Loaded Composite Structures using Passive Thermography. Sensors 2018, 18(10), 3562; doi:10.3390/s18103562.
[7] Winfree, W. P., Zalameda, J. N., and Michael R. Horne, "Simulations of Thermal Signatures of Damage Measured during Quasi-Static Loading of a Single Stringer Panel", manuscript submitted for publication in the 45th Annual Review of Progress in Nondestructive Evaluation, Burlington, VT, USA, 14-20 July 2018.
[8] Avdelidis, N. P., Exarchos, D., Vazquez, P., Ibarra-Castanedo, C., Sfarra, S., Maldague, X., and Matikas, T. E., "Fracture Behavior of Reinforced Aluminum Alloy Matrix Composites using Thermal Imaging Tools", Proceedings Volume 9861, Thermosense: Thermal Infrared Applications XXXVIII; 98610K (2016), doi:10.1117/12.2225511.
[9] Chan, M., (published 2012, March 09), "Perspective Control/Correction", Retrieved from URL https://www.mathworks.com/matlabcentral/fileexchange/35531-perspective-control--correction (downloaded Jan. 2018).
[10] Winfree, W.P., Heath, D.M. Thermal diffusivity imaging of aerospace materials and structures. In Proceedings of the Aerospace/Defense Sensing and Controls, Orlando, FL, USA, 13–17 April 1998; pp. 282–290.
[11] Parker, W. J., Jenkins, R. J., Butler, C. P., and Abbott, G., *Journal of Applied Physics*, Vol. 32, September 1961, pp. 1679-1684.
[12] Weisstein, Eric W., "Levenberg-Marquardt Method." From *MathWorld*--A Wolfram Web Resource. http://mathworld.wolfram.com/Levenberg-MarquardtMethod.html.